Interleukin-6-depedent epithelial fluidization initiates fibrotic lung remodeling

Jacob E. Michalski[1*], Ian T. Stancil[1*], Corinne E. Hennessy[1], Kristina L. Hatakka[1], Ivana V. Yang[1,2], Jonathan S. Kurche[1], Mercedes Rincon[3], and David A. Schwartz[1,3] (*Contributed equally)

[1] Department of Medicine, Division of Pulmonary Sciences and Critical Care Medicine, University of Colorado Anschutz Medical Campus
[2] Department of Medicine, Division of Biomedical Informatics and Personalized Medicine, University of Colorado Anschutz Medical Campus
[3] Department of Immunology and Microbiology, University of Colorado Anschutz Medical Campus

Within the lung, distal airspace remodeling in both:

- Acute lung injury → viral infection
- Chronic lung disease → idiopathic pulmonary fibrosis (IPF)

Results formation of "bronchiolized" regions and honeycomb cyst formation at the expense of gas-exchange units

What are the dynamic and signaling mechanisms regulating this remodeling?

IPF Honeycomb Cyst

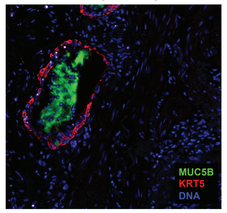

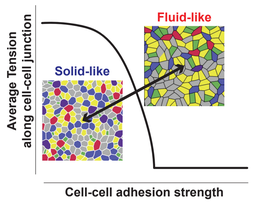

Epithelia can transition between solid-like to fluid-like phases

- Characterized by ability to collectively migrate and distinct changes in cell shape
- Distinct from wound healing or EMT
- Involved in tissue-level remodeling in development

Are airway epithelial phase transitions involved in lung remodeling?

Epithelial cells obtained from explanted IPF lungs (N=5)

Isolated from multiple regions per subject

- Proximal airways (N=5)
- Distal airways (N=5)
- Honeycomb cysts (N=4)

All cells cultured identically, used at passage ≦2 at air-liquid interface (ALI)

- Basa cell surface = media
- Apical cell surface = air
- Robust replication of in vivo phenotypes by day 14 of ALI

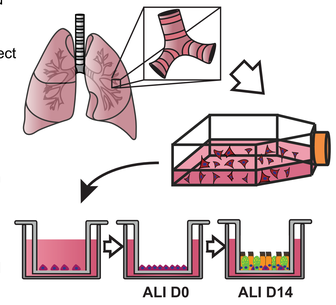

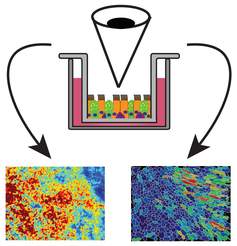

Phase dynamics of epithelia culture at ALI assessed by:

Time lapse microscopy →
- Cell speed
- Root mean-squared velocity (V_{RMS})

F-actin labeling of cell shape →
- Shape index (q) = perimeter/√area
- Cell aspect ratio

Analysis using open-source software
- ImageJ
- PIVLab (MATLAB)
- SeedWater Segmenter (Python)

IL-6-Related Activation

Proximal airway cultures treated at day 14 of ALI with:

- **IL-6 + soluble IL-6R (sIL-6Ra)**
- **IL-11**
- **Oncostatin-M (OSM)**

IL-6-Related Inhibition

Distal airway and honeycomb cultures treated at day 14 of ALI with:

- **Anti-IL-6R antibody**
- **Ruxolitinib (JAK1/2 inhibitor)**
- **Saracatinib (SFK inhibitor)**

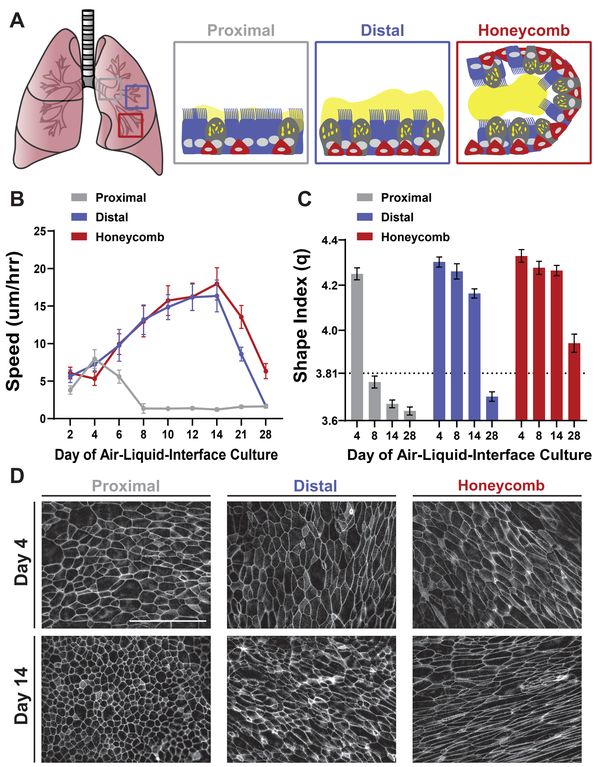

Figure 1: Phase dynamics in IPF airway epithelia diverge along proximal-distal axis. (A) Schematic of represented regions of IPF airway epithelia: proximal, distal, and honeycomb cyst. **(B)** IPF proximal airways undergo migratory to non-migratory shift at day 8 of ALI, whereas distal and honeycomb epithelia remain migratory until day 28 of ALI. Shown: mean cell speed with error bars representing 95% confidence interval. **(C)** IPF proximal airways undergo shift from elongated, pentagonal to hexagonal cell shape at day 8 of ALI, whereas distal and honeycomb epithelia remain persistently elongated. Shown: mean cell shape index (q) with q=3.81 representing predicted shift between solid and fluid phases, error bars represent 95% confidence intervals. **(D)** Representative F-actin labelled cell borders at days 4 and 14 of ALI in proximal, distal, and honeycomb cultures demonstrating cell shape changes in proximal cultures but persistent elongated cell shape in distal and honeycomb regions. Scale bar represents 100 um.

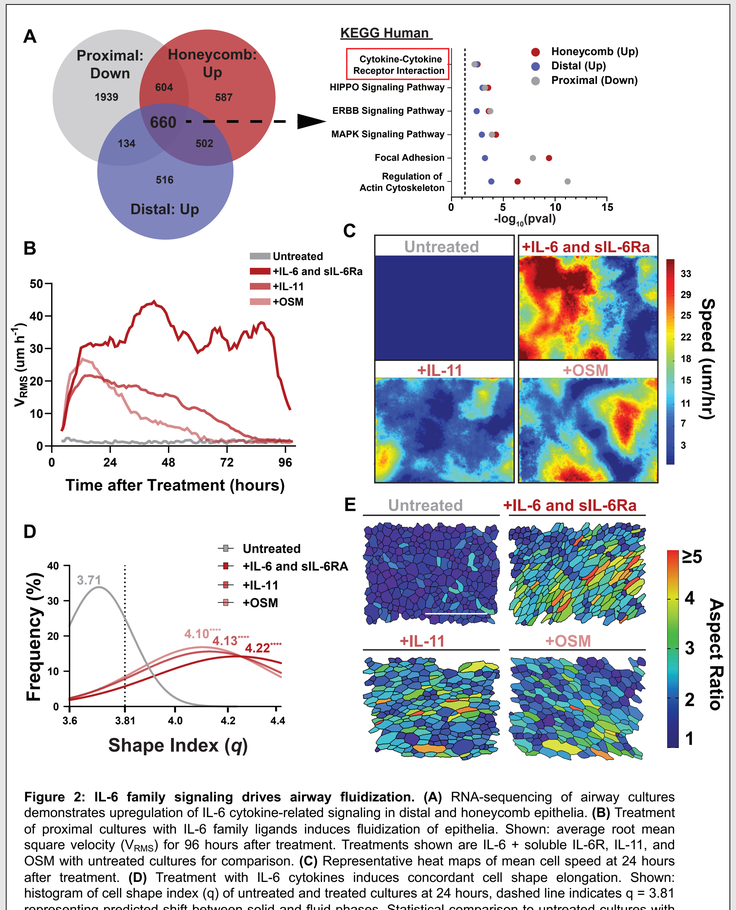

Figure 2: IL-6 family signaling drives airway fluidization. (A) RNA-sequencing of airway cultures demonstrates upregulation of IL-6 cytokine-related signaling in distal and honeycomb epithelia. **(B)** Treatment of proximal cultures with IL-6 family ligands induces fluidization of epithelia. Shown: average root mean square velocity (V_{RMS}) for 96 hours after treatment. Treatments shown are IL-6 + soluble IL-6R, IL-11, and OSM with untreated cultures for comparison. **(C)** Representative heat maps of mean cell speed at 24 hours after treatment. **(D)** Treatment with IL-6 cytokines induces concordant cell shape elongation. Shown: histogram of cell shape index (q) of untreated and treated cultures at 24 hours, dashed line indicates q = 3.81 representing predicted shift between solid and fluid phases. Statistical comparison to untreated cultures with one-way ANOVA test, *p<0.05, **p<0.01, ***p<0.001, ****p<0.0001. **(E)** Representative segmented images of F-actin-stained cell borders in untreated and IL-6 stimulated cultures. Color-coding represents individual cell aspect ratio. Scale bar represents 100 um.

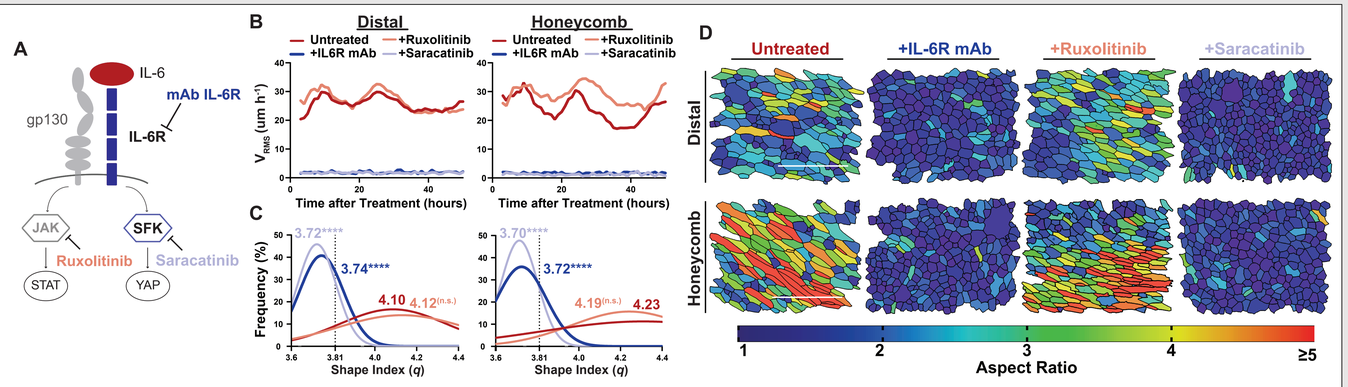

Figure 3: Inhibition of IL-6/SFK axis attenuates epithelial fluidization. (A) Schematic of IL-6 signaling through downstream JAK1/2 or SRC family kinases (SFK) with utilized inhibitors noted. **(B)** Blockade of IL-6R or SFK, but not JAK1/2, prevents epithelial fluidization. Shown: average root mean square velocity (V_{RMS}) of distal and honeycomb cultures for 48 hours after treatment. Treatments shown are anti-IL-6R antibody, ruxolitinib (JAK1/2 inhibitor), and saracatinib (SFK inhibitor). **(C)** IL-6R and SFK inhibition induce concordant cell shape change in fluidized distal and honeycomb epithelia. histogram of cell shape index (q) of untreated and treated cultures at hours, dashed line indicates q = 3.81 representing predicted shift between solid and fluid phases. Statistical comparison to untreated cultures with one-way ANOVA test, (n.s) not significant, *p<0.05, **p<0.01, ***p<0.001, ****p<0.0001. **(D)** Representative segmented images of F-actin-stained cell borders in untreated and inhibited cultures. Color-coding represents individual cell aspect ratio. Scale bar represents 100 um.

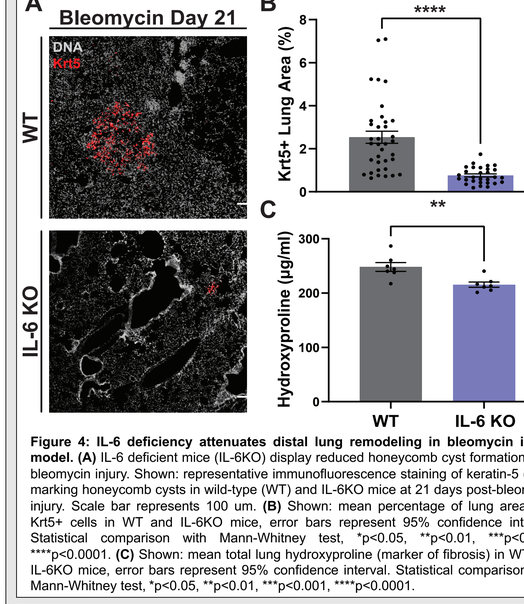

Figure 4: IL-6 deficiency attenuates distal lung remodeling in bleomycin injury model. (A) IL-6 deficient mice (IL-6KO) display reduced honeycomb cyst formation after bleomycin injury. Shown: representative immunofluorescence staining of keratin-5 (Krt5) marking honeycomb cysts in wild-type (WT) and IL-6KO mice at 21 days post-bleomycin injury. Scale bar represents 100 um. **(B)** Shown: mean percentage of lung area with Krt5+ cells in WT and IL-6KO mice, error bars represent 95% confidence interval. Statistical comparison with Mann-Whitney test, *p<0.05, **p<0.01, ***p<0.001, ****p<0.0001. **(C)** Shown: mean total lung hydroxyproline (marker of fibrosis) in WT and IL-6KO mice, error bars represent 95% confidence interval. Statistical comparison with Mann-Whitney test, *p<0.05, **p<0.01, ***p<0.001, ****p<0.0001.

Summary of Additional Findings

Airway epithelia are fluidized in in vivo mouse lung injury models

- Bleomycin, influenza (H1N1 PR8)

Pharmacologic inhibition of IL-6/SFK signaling axis prevents epithelia from becoming fluidized

Mesenchymal cells from fibrotic lungs express higher levels of IL-6-family cytokines

Healthy epithelia co-cultured with fibrotic mesenchymal cells become fluidized

- Can be rescued by blocking IL-6 signaling

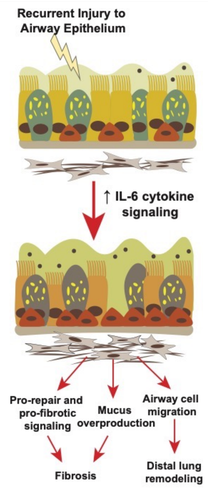

IPF airway epithelia display aberrant phase dynamics

- Specific to the distal airways and honeycombed regions

Fluid-to-solid phase transitions can be modulated by IL-6-related signaling

- Downstream signaling is dependent on SFK but not JAK1/2

Fluidization and signaling mechanisms are conserved in mouse lung injury models

Targeting IL-6 signaling attenuates "honeycomb-like" cyst formation and fibrosis in mouse bleomycin model

Distal airway is an initiator in fibrotic lung disease

- **In contrast to the focus of the field on fibroblasts and alveolus**

This research was supported by the following funding: NIH-NHLBI (UG3/UH3-HL151865), DoD Focused Program Project (W81XWH-17-1-0597), NIH-NHLBI (R01-HL149836), VAMC Merit Review (IO1BX005295), NIH-NHLBI (P01-HL0928701), NIH-NHLBI (UH2/3-HL123442), NIH-NHLBI (X01-HL134585), and NIH-NIA (T32-AG000279).